

Experimental Observation on Bond-Slip Behavior between Concrete and CFRP Plate

Dong-Suk Yang¹⁾, Sung-Nam Hong²⁾, and Sun-Kyu Park^{2)*}

(Received November 22, 2006, Accepted May 30, 2007)

Abstract: This paper discusses the failure mode of reinforced concrete beams strengthened with composite materials based on six experimental set-ups to determine the FRP-to-concrete bond strength. Interfacial bond behavior between concrete and CFRP plates was discussed. Shear test were performed with different concrete compressive strengths (21 MPa and 28 MPa) and different bonding length (100 mm, 150 mm, 200 mm, and 250 mm). Shear test results indicate that the effective bond length (the bond length beyond which the ultimate load does not increase) was estimated as 196~204 mm through linear regression analysis. Failure mode of specimens occurred due to debonding between concrete and CFRP plates. Maximum bond stress is calculated as about 3.0~3.3 MPa from the relationships between bond stress and slip. Finally, the interfacial bond-slip model between CFRP plates and concrete, which is governed debonding failure, has been estimated from shear tests. Average bond stress was about 1.86~2.04 MPa, the volume of slip between CFRP plate and concrete was about 1.45~1.72 mm, and the fracture energy was found to be about 1.35~1.71 N/mm.

Keywords: bond-slip model, bond strength, CFRP plate, debonding, shear test

1. Introduction

The use of FRP in upgrading and strengthening civil concrete structures has been accepted gradually only in recent years. In the past, FRP materials were used primarily in the aerospace and defence industries rather than in civil construction areas, mainly due to the prohibitively high cost of raw materials and manufacturing processes. Previous research showed that fiber composites could be effectively used for the strengthening of concrete beam resulting in the improvement of flexural load carrying capacity. Among all different types of concrete strengthening methods, the use of FRP materials for strengthening concretes under tensile stresses presents better strengthening characteristic in terms of the ultimate flexural load capacity.^{1,6,9,10,15}

Based on existing studies, a schematic representation of seven typical failure modes observed in test is shown in Table 1.¹⁶ These seven failure modes are termed (a) flexural failure by FRP rupture; (b) flexural failure by crushing of compressive concrete; (c) shear failure; (d) concrete cover separation; (e) plate end interfacial debonding; (f) intermediate flexural crack induced interfacial debonding; and (g) intermediate flexural-shear crack induced interfacial debonding. Tests have shown that the load-

carrying capacity of RC beams flexurally-strengthened with a FRP plate bonded to the tension face is often limited by one of the debonding failure modes.¹⁸

This paper presents interfacial bond behavior between concrete and CFRP plates in shear. Shear test were performed with different concrete compressive strengths (21 MPa and 28 MPa) and different bonding length (100 mm, 150 mm, 200 mm and 250 mm) as main experimental variables. The effective bond length has been estimated in accordance with concrete compressive strength using a linear regression analysis. Maximum bond stress and slip are calculated from strain of CFRP plates by load step. Finally, the interfacial bond-slip model between CFRP plates and concrete, which is governed debonding failure, has been estimated from shear tests.

2. Shear test methods

A recent survey showed that many different experimental set-ups have been used for determining the FRP-to-concrete bond strength, but no consensus on a standard test procedure has been reached. Chen et al. classified the existing test set-ups into the following five types¹⁹: (a) double-shear pull tests; (b) double-shear push tests; (c) single-shear pull tests; (d) single-shear push tests; and (e) beam (or bending) tests. For better clarity, the first four test methods are renamed here as: (a) far end supported (FES) double-shear tests; (b) near end supported (NES) double-shear tests; (c) far end supported (FES) single-shear tests; and (d) near end supported (NES) single-shear tests (Table 2). Collectively, all these four tests may also be referred to as pull tests, as the plate is always directly pulled by tensile force.

¹⁾KCI Member, Dept. of Civil Engineering, University of Sherbrooke, Canada.

²⁾KCI Member, Dept. of Civil Engineering, Sungkyunkwan University, Suwon 440-330, Korea.

³⁾KCI Member, Dept. of Civil Engineering, Sungkyunkwan University, Suwon 440-330 Korea. E-mail : skpark@skku.edu

Copyright © 2007, Korea Concrete Institute. All rights reserved, including the making of copies without the written permission of the copyright proprietors.

Table 1 Failure modes of RC beams strengthened by FRP.

Modes	Shape
FFF ¹⁾	
FFC ²⁾	
SF ³⁾	
CCS ⁴⁾	
EID ⁵⁾	
IFC ⁶⁾	
IFS ⁷⁾	

- ¹⁾ Flexural failure by FRP rupture
- ²⁾ Flexural failure by crushing of compressive concrete
- ³⁾ Shear failure
- ⁴⁾ Concrete cover separation
- ⁵⁾ End interfacial debonding
- ⁶⁾ Intermediate flexural crack induced interfacial debonding
- ⁷⁾ Intermediate flexural-shear crack induced interfacial debonding

3. Shear test

3.1 Materials and specimens

A total of 8 specimens were tested in shear test. The specimen size was a rectangular section of 100 mm × 100 mm × 300 mm (width × height × length). In order to apply tensile force, concrete blocks of same size are inserted into each end. The material properties of CFRP plates are given in Table 3.

One of the blocks had only the bonded CFRP laminates, while the other was consisted of a similarly bonded CFRP laminate with an additional CFRP sheet wrap to prevent debonding from this block. Strains and slips were not measured for this second block. The main experimental variables were, bonding length of CFRP plates (100 mm, 150 mm, 200 mm, and 250 mm) and concrete compressive strength (21 Mpa and 28 MPa). Details of specimens are provided in Table 4. Here, the thickness of resin is about 3 mm and the width of CFRP plate in shear test is 50 mm.

Table 2 Classification of bond test.

Kinds	Shape
Far-end supported double-shear test	
Near-end supported double-shear test	
Far-end supported single-shear test	
Near-end supported single-shear test	
Beam test	
Modified beam test	

Table 3 Material properties of CFRP plate.

	Tensile strength (MPa)	Modulus of elasticity (MPa)	Remarks
CFRP plates	2,350	1.73 × 10 ⁵	Width : 50 mm Thickness : 1.3 mm
Epoxy resin	33.5	1,500–3,500	Bond strength : 4.3 MPa

Table 4 Details of specimens.

Specimens	Epoxy thickness (mm)	Bond width (mm)	Concrete compressive strength (MPa)	Bond length (mm)
D21-10	3.0	50	21	100
D21-15				150
D21-20				200
D21-25				250
D28-10			28	100
D28-15				150
D28-20				200
D28-25				250

3.2 Loading equipment and arrangement of strain gauges

In order to measure the strains in the CFRP laminates during loading, strain gauges have been bonded to the CFRP plates as shown in Fig. 1. CFRP plates were attached at both sides of specimens, so that the mean value of the strains could be obtained. Loading was increased monotonically. Because the bond strength was small, the velocity of loading should be as low as possible. The data were automatically collected by the

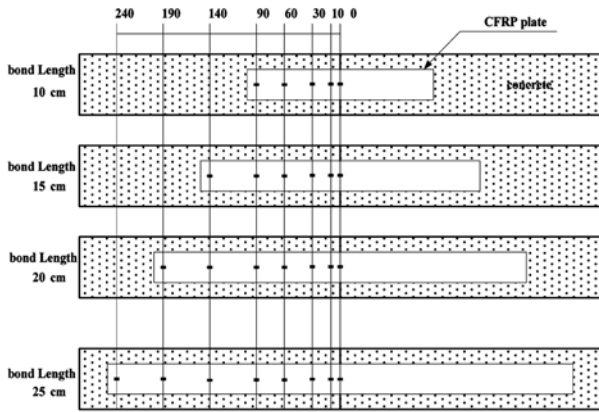


Fig. 1 Location of strain gauge (unit : mm).

automatic data logger system.

As shown in Fig. 2, rebar has been inserted in both sides of specimen for tensile loading to minimize eccentric loading. In addition, LVDT was attached to each side of the specimen in order to measure possible slip during loading.

4. Results and discussion

4.1 Test results

The shear test results of 8 specimens having 100 mm, 150 mm, 200 mm, and 250 mm of bond lengths are shown in Table 5.

The maximum load increased as the bond length increases. The effective bond length at which the maximum load does not increase from a certain bond length was also estimated with linear regression analysis as shown in Fig. 3. From Fig. 3 it could be concluded that it is suitable to take the effective bond length as about 196–204 mm. Regardless of concrete compressive strength, average bond stress decreases until effective bond length and average bond stress become constant when the bond length is greater than the effective bond length.

4.2 Relationships between loads and cfrp plates strains

In order to measure the strain gradient along the bond length of CFRP plates, strain gauges were attached as shown in Fig. 1. Failure of specimens occurred due to debonding between concrete

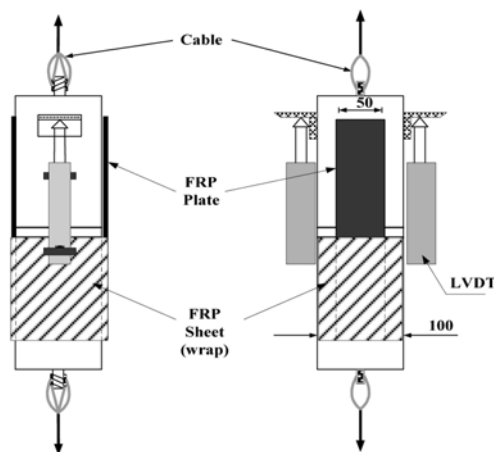
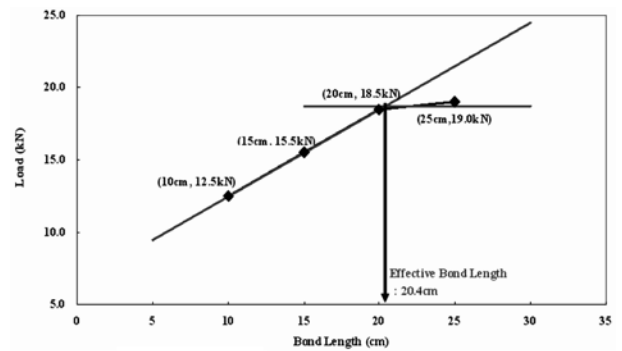


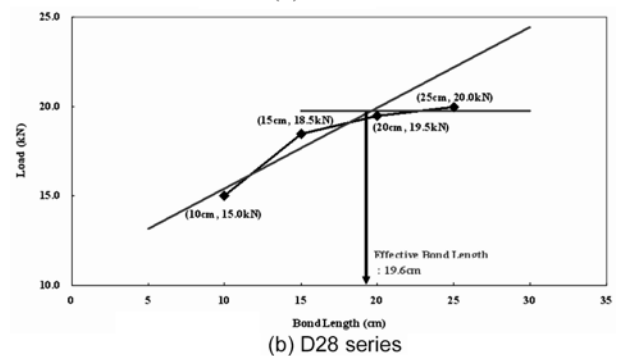
Fig. 2 Loading of specimens.

Table 5 Results of shear test.

Specimens	Cracking load (kN)	Ultimate load (kN)	Effective bond length (mm)	Average bond stress (MPa)
D21-10	12.5	12.5	-	2.50
D21-15	15.5	15.5	-	2.07
D21-20	18.5	18.5	204	1.85
D21-25	19.0	22.5	204	1.86
D28-10	15.0	15.0	-	3.00
D28-15	18.5	18.5	-	2.47
D28-20	19.5	19.5	196	1.99
D28-25	20.0	21.5	196	2.04



(a) D21 series



(b) D28 series

Fig. 3 Estimation of effective bond length.

and CFRP plates as shown in Fig. 4, and relationships between load and CFRP plates strain are shown in Fig. 5.

As shown in Fig. 5, the stress is concentrated in the loading point and the strain increases uniformly in the initial load stage. However, load is transferred to CFRP plate interior as the load increases. Therefore, the strain will increase until specimen is debonded. In particular, strain increases linearly in the region where the gages were attached during the initial load in specimens D21-20, D21-25, D28-20 and D28-25. However, it

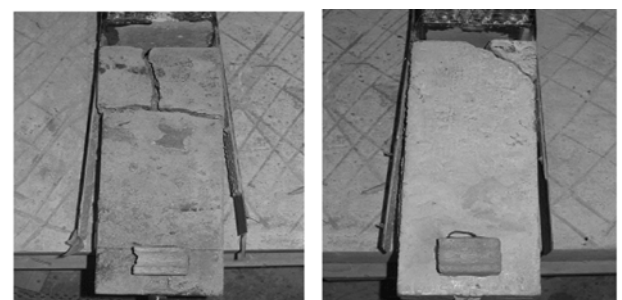


Fig. 4 Failure modes of specimens in shear test.

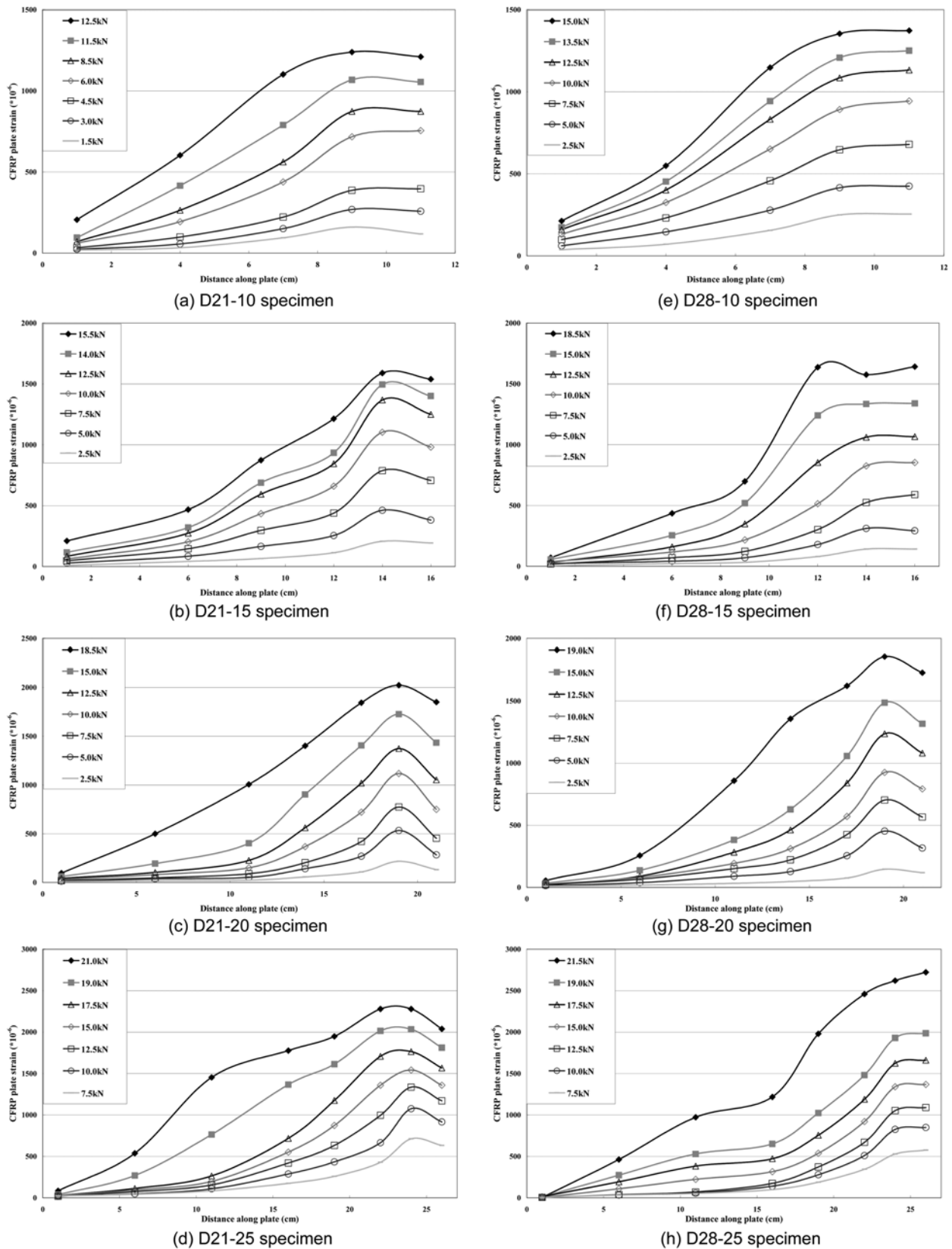


Fig. 5 Relation of load and CFRP plates in shear test.

has been observed that the strain rapidly changes before CFRP plate debonding. Therefore, it could be concluded that it is suitable to take the effective bond length as about 200 mm.

4.3 Calculation of bond stress and slip

Degree of freedom in interface element between CFRP plates

and concrete is shown in Fig. 6(a).

The relation among tensile load $A_f f_f$, bond stress τ_b , and element of length dx are obtained from the equilibrium of element in Fig. 6 (b). From equilibrium conditions,

$$A_c df_c + A_f df_f = 0 \quad (1)$$

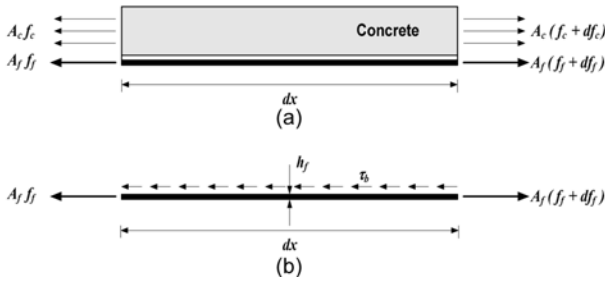


Fig. 6 Bond stress between CFRP plates and concrete.

$$\tau_b(b_f dx) = A_f(f_f + df_f) - A_f f_f \quad (2)$$

where A_c , A_f are cross-section area of concrete and FRP material respectively, and b_f , f_f are width and tensile stress of FRP material.

Bond stress (τ_b) can be arranged as follows using Eqs. (1) and (2).

$$\tau_b = h_f \frac{df_f}{dx} = h_f E_f \frac{d\varepsilon_f}{dx} \quad (3)$$

where h_f , E_f and ε_f are thickness, elasticity modulus and strain of FRP material, respectively.

Strain distribution curve of CFRP plate is assumed to be by quadratic from the observation made for CFRP plate strain of interface. If three data points $(x_{i-1}, \varepsilon_{i-1})$, (x_i, ε_i) , $(x_{i+1}, \varepsilon_{i+1})$ are available, fitting equation can be estimated with a second-order equation.

$$\varepsilon_s = \varepsilon(x) = a_i + b_i x + c_i x^2 \quad (4)$$

After substituting the measured three data points $(x_{i-1}, \varepsilon_{i-1})$, (x_i, ε_i) , $(x_{i+1}, \varepsilon_{i+1})$ into Eq. (4), coefficients a_i , b_i , c_i . Bond stress $\tau_{bi}(x)$ can be calculated as can be evaluated.

$$\tau_{bi}(x) = E_f h_f (b_i + 2c_i x) \quad (5)$$

Slip (δ) can be calculated using Eq. (6).

$$\delta_i(x) = \delta_{i-1}(x) + \int_{x_{i-1}}^{x_i} (a_i + b_i x + c_i x^2) dx \quad (6)$$

Bond stress of specimens that is more than bond length 200 mm in shear test in accordance with load step are shown in Figs. 7 and 8. Maximum bond stress is calculated as 3.0~3.3 MPa, slip of specimens with bond length of 200 mm as 0.3~0.42 mm and specimens with bond length of 250 mm as 0.8~1.1 mm.

4.4 Estimation of interfacial bond-slip model

The interfacial bond-slip model between CFRP plates and concrete, which is governed by debonding failure, has been estimated from shear tests. In the structure, because bond length is generally greater than the effective bond length, specimens greater than the effective bond length have been applied (D21-20, D21-25, D28-20, D28-25 specimens).

The important factors of bond-slip model are average bond stress and magnitude of slip. Average bond stress (τ_{ave}) is shown in Table 4. The magnitude of slip (δ), defined as a relative slip between concrete and CFRP plate, is calculated by difference between two displacement of each section of CFRP plates and displacement of concrete.

As shown in Fig. 9, slip (δ) between CFRP plate and concrete was about 1.45~1.72 mm, and the fracture energy (G_f , area under

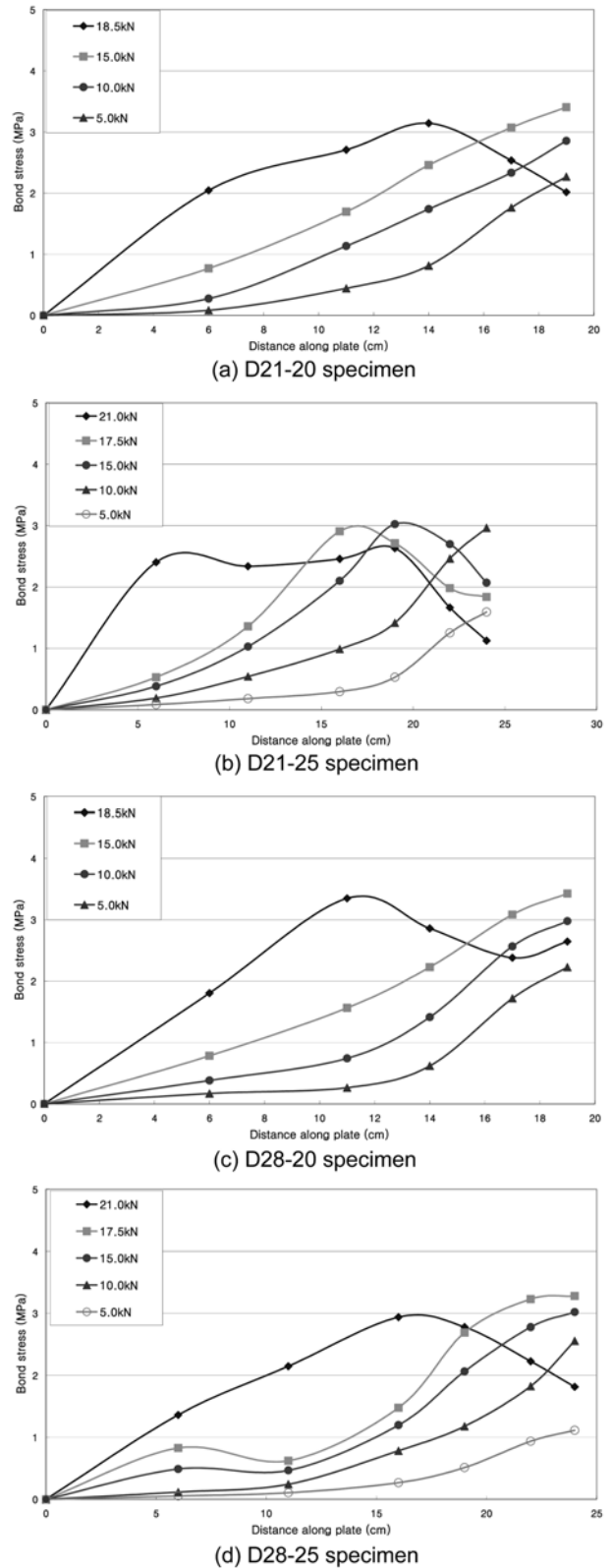
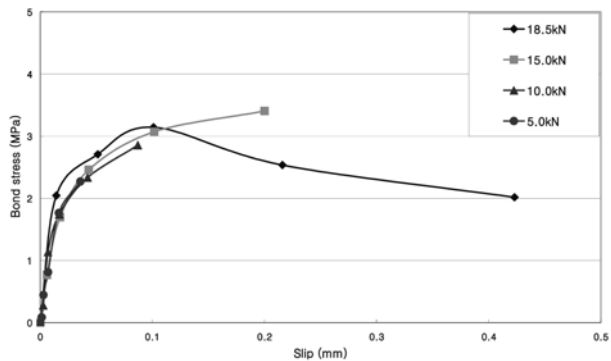


Fig. 7 Bond stress distribution of specimens.

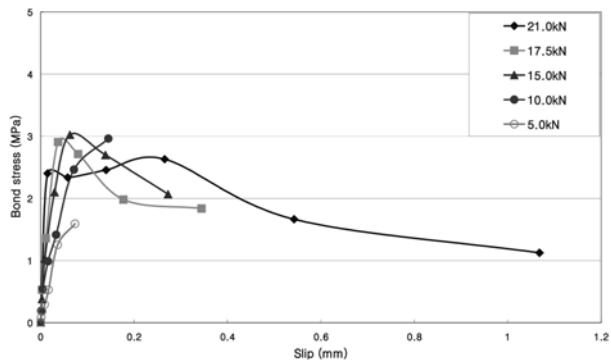
the τ - δ curve) was found to be about 1.35~1.71 N/mm.

5. Conclusions

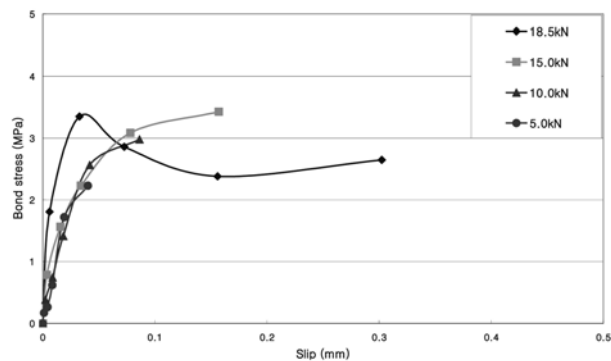
In this paper, shear tests were performed for different the concrete compressive strengths and the bonding lengths. The effective bond length and interfacial bond-slip model between



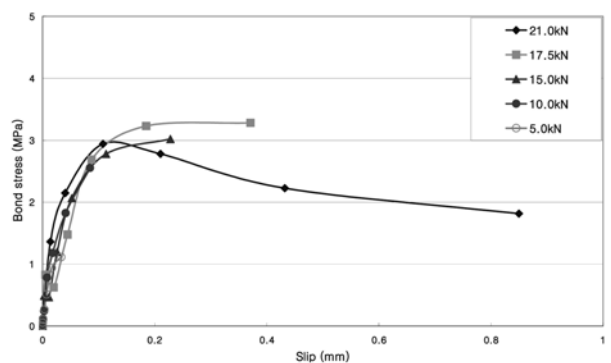
(a) D21-20 specimen



(b) D21-25 specimen



(c) D28-20 specimen



(d) D28-25 specimen

Fig. 8 Bond stress and slip of specimens.

CFRP plates and concrete were estimated in accordance with the concrete compressive strength. The following conclusions were made from this study:

1) The effective bond length at which the maximum load does not increase from a certain bond length was estimated using the linear regression analysis. It could be concluded that it is suitable to take the approximate effective bond length as 200 mm.

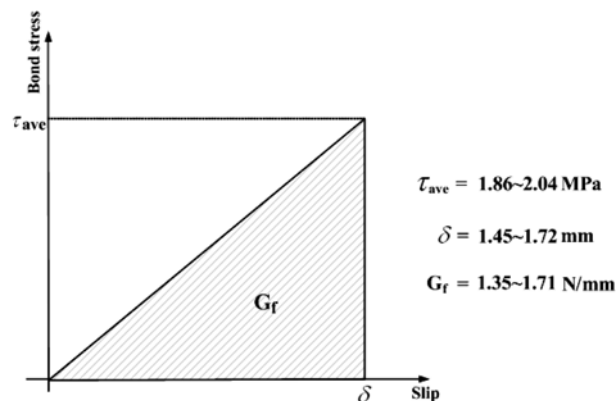


Fig. 9 Estimation of bond-slip model.

2) Failure mode of specimens occurred due to debonding of CFRP plates. The bond stress is concentrated in the loading point and the strain increases uniformly in the initial load stage.

3) Bond stress of specimens with bond length longer than 200 mm was estimated using the basic equation for bond stress and slip. Maximum bond stress was estimated as about 3.0~3.3 MPa.

4) The interfacial bond-slip model between CFRP plates and concrete, which is governed by debonding failure, has been estimated from shear tests. Average bond stress was about 1.86~2.04 MPa, magnitude of slip between CFRP plate and concrete was about 1.45~1.72 mm, and the fracture energy was found to be about 1.35~1.71 N/mm.

Acknowledgements

This work was supported by the Korea Research Foundation Grant funded by the Korean Government (MOEHRD) (KRF-2006-214-D0015).

References

1. Alfarabi, S. A., Al-Sulaimani, G. J., and Basunbul, I. A., "Strengthening of Initially Loaded Reinforced Concrete Beams Using FRP Plates," *ACI Structural Journal*, Vol.91, 1994, pp.160~168.
2. Arduini, M., Tommaso, A., and Nanni, A., "Brittle Failure in FRP Plate and Sheet Bonded Beams," *ACI Structural Journal*, Vol.94, No.4, 1997, pp.363~370.
3. Bizindavyi, L. and Neale, K. W., "Transfer Lengths and Bond Strengths for Composites Bonded to Concrete," *Journal of Composites for Construction, ASCE*, Vol.3, No.4, 1999, pp.153~160.
4. Brosens, K. and Gemert, D., "Anchoring Stresses between Concrete and Carbon Fibre Reinforced Laminates," *Proceedings of the Third International Symposium on Non-metallic (FRP) Reinforcements for Concrete Structures*, Sapporo, Vol.1, 1997, pp.271~278.
5. Chen, J. F. and Teng, J. G., "Anchorage strength models for FRP and Steel Plates Bonded to Concrete," *Journal of Structural Engineering*, Vol.127, No.7, 2001, pp.784~791.
6. Fanning, P. J. and Kelly, O., "Ultimate Response of RC Beams Strengthened with CFRP Plates," *Journal of Composites*

for Construction, ASCE, Vol.5, No.2, 2001, pp.122~127.

7. KICT, *Development of New Technology on Strengthening RC Structures with Externally Post-Tensioning CFRP Strips (1st Year)*, Korea Institute of Construction Technology, 2004, In Korean.

8. Mander, J. B., Priestley, M. J., and Park, R., "Theoretical Stress-strain Model for Confined Concrete," *Journal of Structural Engineering*, ASCE, Vol.114, No.8, 1988, pp.1804~1849.

9. Malek, A. M., Saadatmanesh, H., and Ehsani, M. R., "Prediction of Failure Load of R/C Beams Strengthened with FRP Plate due to Stress Concentration at the Plate End," *ACI Structural Journal*, Vol.95, No.1, 1998, pp.142~152.

10. Michel, J., Chajes, T. F., Januszka, D. R., Mertz, T. A., Thomson, J. R., and Willam W. F., "Shear Strengthening of Reinforced Concrete Beams Using Externally Applied Composite Fabrics," *ACI structural Journal*, 1995, pp.295~303

11. Mukhopadhyaya, P. and Swamy, R. N., "Interface Shear Stress: a New Design Criterion for Plate Debonding," *Journal of Composites for Construction*, ASCE, Vol.5, No.1, 2001, pp.35~43.

12. Naaman, A. E. and Alkhairi, F. M., "Stress at Ultimate in Unbonded Post-tensioning Tendon: Part 2-Proposed Methodology," *ACI Structural Journal*, Vol.88, No.6, 1991, pp.683~690.

13. Oehlers, D. J., "Reinforced Concrete Beams with Plates Glued to Their Soffits," *Journal of Structural Engineering*,

ASCE, Vol.118, No.8, 1992, pp.2023~2038.

14. Park, S. K. and Yang, D. S., "Flexural Behavior of Reinforced Concrete Beams with Cementitious Repair Materials," *Materials and Structures*, Vol.38, 2005, pp.329~334

15. Rahimi, H. and Hutchinson, A., "Concrete Beams Strengthened with Externally Bonded FRP Plates," *Journal of Composites for Construction*, ASCE, Vol.5, No.1, 2001, pp.44~56.

16. Smith, S. T. and Teng, J. G., "FRP-Strengthening RC Beams, II: Assessment of Debonding Strength Models," *Engineering Structures*, Vol.24, 2002, pp.397~417.

17. Smith, S. T. and Teng, J. G., "Shear-Bending Interaction In Debonding Failures of FRP-Plated RC Beams," *Advanced Structure Engineering*, Vol.6, No.3, 2003, pp.183~200.

18. Teng, J. G., Smith, S. T., Yao, J., and Chen, J. f., "Intermediate Crack-induced Debonding in RC Beams and Slabs," *Construction and Building Materials*, 2003, pp.447~462.

19. Yao, J., Teng, J. G., and Chan, J. F., "Experimental Study on Frp-to-concrete Bonded Joints," *Composites Part B-Engineering*, Vol.36, 2005, pp.99~113.

20. Ziraba, Y. N., Baluch, M. H., Basunbul, A. M., Sharif, I. A., Azad, A. K., and Al-Sulaimani, G. J., "Guidelines Towards the Design of Reinforced Concrete Beams with External Plates," *ACI structural Journal*, Vol.91, No.6, 1994, pp.639~646.